polymer papers

Experimental investigations of light scattering by polystyrene–poly(methyl methacrylate)–good solvent and polystyrene–poly(vinyl acetate)–good solvent

Latifa Ould-Kaddour* and Claude Strazielle†
Institut Charles Sadron (CRM-EAHP), CNRS-ULP, 6 rue Boussingault, 67083 Strasbourg-cedex, France
(Received 18 October 1990; revised 22 February 1991; accepted 22 February 1991)

Experimental investigations of light scattering are presented for two ternary systems (two chemically different polymers with a solvent): polystyrene(PS)–poly(methyl methacrylate)(PMMA)–benzene (or toluene) and PS–poly(vinyl acetate)(PVAc)–styrene. These systems show similarities with respect to the incompatibility between the two unlike polymers. Experiments are reported for mixtures with different molecular weights and for concentrations ranging from dilute solution to the onset of phase separation. Thermodynamic analysis is undertaken by evaluating the polymer–polymer interaction parameters. For both systems, the polymer–polymer interaction parameters are constant in dilute solution but increase in the semi-dilute regime. A more complete study is performed on the PS–PMMA–toluene system by analysing the angular distribution of the scattered intensity.

(Keywords: light scattering; ternary systems; interaction parameters)

INTRODUCTION

Since early theoretical and experimental work on ternary systems (polymer A–polymer B–solvent S) light scattering methods[1–4] have been primarily used for investigating the thermodynamic properties between two unlike polymers.

Recently, more complete experimental studies of light scattering on ternary systems were reported. They also concerned the influence of thermodynamic and molecular properties on the angular distribution of the scattered intensity. These systems were: polystyrene(PS)–polydimethylsiloxane(PDMS)–good solvent[5], PS–polyvinylmethylether(PVME)–good solvent[6] and PDMS–poly(methyl methacrylate)(PMMA)–good solvent[7]. They differ in the thermodynamic behaviour of the two polymers. The results have been analysed using recent theories[8,9]. In this work, we propose to extend such investigations to two other ternary systems characterized by the same degree of incompatibility, namely: PS–PMMA–benzene or toluene and PS–poly(vinyl acetate)(PVAc)–styrene.

The solvents used for the first system have the same refractive index as PMMA. Hence one 'sees' only the PS, and thus data interpretation is simpler. The styrene in the other system is also a special optical solvent, because it gives 'an average contrast' equal to zero.

In this paper, the theoretical formalism to be used for data interpretation is summarized, samples and experimental techniques are described, and a thermodynamic study is presented for both systems by analysing the scattered intensity at wavevector equal to zero. Finally, a more detailed study is extended to the angular distribution of the scattered intensity in a large wavevector range for the PS–PMMA–toluene system.

THEORETICAL

The general relation for the excess scattered intensity by a mixture of two polymers A and B with a solvent S is given by the following equation:

$$\Delta I \simeq \frac{a^2 x_a + b^2 x_b + (a^2 v_b + b^2 v_a - 2ab v_{ab}) x_a x_b}{1 + v_a x_a + v_b x_b + (v_a v_b - v_{ab}^2) x_a x_b} \quad (1)$$

for all concentrations and wavevectors q [$=(4\pi/\lambda)\sin(\theta/2)$ where λ is the wavelength of the incident beam in the medium and θ is the scattering angle]. In equation (1), a and b are the contrast factors, which are identified with the refractive index increments, $v_a = dn/dc_a$ and $v_b = dn/dc_b$, of the two polymers, respectively. The terms v_a, v_b and v_{ab} are the excluded volume parameters which are related to the interactions of polymer A–solvent, polymer B–solvent and polymer A–polymer B in that solvent. The quantities x_i are defined as:

$$x_i = N_i n_i^2 P_i \qquad i = a \text{ or } b \quad (2)$$

where N_i is the number of chains of polymer i per unit volume and n_i the number of elements (or monomers) per chain of polymer i. The number n_i is equal to $M_i \tilde{v}_i / V_S$,

* Present address: University of Tlemcen, BP 119, Tlemcen, Algeria
† To whom correspondence should be addressed

0032-3861/92/050899-10

where M_i and $\tilde{v}_i$ are the molecular weight and the specific volume of polymer i, respectively, and V_S is the molar volume of the solvent. $P_i(q)$ is the form factor of polymer i normalized as $P_i = 1$ for $q = 0$. Its expression for low q values is:

$$P_i(q) = 1 - q^2 R_{g,i}^2/3 \tag{3}$$

where $R_{g,i}$ is the radius of gyration of molecule i.

The general equation (1) is now applied to special experimental conditions.

Conditions in which b = 0 ($dn/dc_b = 0$). If the solvent and polymer B have the same refractive index ($b = 0$), relation (1) is simplified and, using classical variables such as the concentration c_i (in g ml^{-1}), the molecular weight M_i, and the generalized virial coefficients $A_{2,i}$ (i = a or b) and $A_{2,ij}$ (i = a and j = b), one obtains:

$$K'\Delta I(c,q) = \frac{a^2 M_a c_a P_a + 2a^2 A_{2,b} M_a M_b c_a c_b P_a P_b}{1 + 2A_{2,a} M_a c_a P_a + 2A_{2,b} M_b c_b P_b + 4(A_{2,a}A_{2,b} - A_{2,ab}^2) M_a M_b c_a c_b P_a P_b} \tag{4}$$

where $K' = 2\pi^2 n^2/\lambda_0^4 N_a$, K' being the optical constant, λ_0 the wavelength of the incident radiation in vacuum, n the refractive index of the solution and N_a the Avogadro number.

The generalized virial coefficients can be defined in terms of Flory's interaction parameters χ_i (i = a or b) and χ_{ij} (i = a and j = b):

$$A_{2,i} = \frac{\tilde{v}_i^2}{2V_S}\left(\frac{1}{\varphi_S} - 2\chi_i\right) \qquad i = \text{a or b}$$

$$A_{2,ij} = \frac{\tilde{v}_i \tilde{v}_j}{2V_S}\left(\frac{1}{\varphi_S} - \chi_i - \chi_j + \chi_{ij}\right) \qquad i = \text{a and } j = \text{b} \tag{5}$$

where φ_S is the volume fraction of solvent ($= 1 - \varphi_a - \varphi_b$, with $\varphi_a = c_a\bar{v}_a$ and $\varphi_b = c_b\bar{v}_b$).

Therefore equation (4) written in the reciprocal form after some straightforward arrangements gives:

$$\frac{Kc_aM_a}{\Delta I(q)} = \frac{1}{P_a} + 2A_{2,a}M_ac_a - \frac{4A_{2,ab}^2 M_aM_bc_ac_bP_b}{1 + 2A_{2,b}M_bc_bP_b} \tag{6}$$

where $K = K'a^2$.

Wavevector q = 0. At the zero q limit, the form factor P_i tends to unity (see equation (3)), and consequently equations (4) and (6) will depend only on the interaction parameters, the molecular weights and the concentrations. At the spinodal, which corresponds to the metastable state between the homogeneous solution and the demixed phase for an incompatible system, the scattered intensity diverges, i.e. $\Delta I(c, q = 0) \to \infty$. The denominator in equation (4) tends to zero, leading to the characteristic equation of the spinodal:

$$1 + 2A_{2,a}M_ac_a^{sp} + 2A_{2,b}M_bc_b^{sp} + 4(A_{2,a}A_{2,b} - A_{2,ab}^2)M_aM_bc_a^{sp}c_b^{sp} = 0 \tag{7}$$

where c_a^{sp} and c_b^{sp} are the concentrations of polymers A and B at the spinodal, respectively.

Dilute solution ($dn/dc_a = -dn/dc_b$). If we apply the general equation (1) to dilute solution, i.e. keeping terms up to second order in concentration, we obtain:

$$\Delta I(c,q) \simeq a^2x_a + b^2x_b - 2abv_{ab}x_ax_b - a^2v_ax_a^2 - b^2v_bx_b^2 + \cdots \tag{8}$$

Assuming that:

$$v_a + v_b - 2v_{ab} = -\frac{2V_S}{N_a}\chi_{ab} \tag{9}$$

equation (8) is written as:

$$\Delta I(c,q) \simeq a^2x_a + b^2x_b - \frac{2V_S}{N_a}ab\chi_{ab}x_ax_b - (ax_a + bx_b)(ax_av_a + bx_bv_b) \tag{10}$$

If the refractive index increment of the two polymers and their concentrations are such that:

$$ax_a + bx_b = 0 \tag{11}$$

the third term of equation (10) vanishes. From the measurements of the scattered intensity, one can determine the interaction parameter χ_{ab} with good precision, without knowing $A_{2,a}$ and $A_{2,b}$ (or χ_a and χ_b). The condition (11) is known as the 'null average contrast' condition and can be fulfilled by choosing solvent and concentrations such that: $b = -ax_a/x_b$, i.e. by finding a solvent in which a and b are of opposite sign. This method was suggested and used by Fukuda *et al.*[10].

A further simplification arises when the wavevector q is equal to zero. Then relation (10) is:

$$\frac{K'c_t}{\Delta I(c_t, q = 0)} = A + BA^2c_t \tag{12}$$

$$A = [a^2M_ay + b^2M_b(1 - y)]^{-1}$$

$$B = 2abM_aM_by(1 - y)\frac{\tilde{v}_a\tilde{v}_b}{V_S}\chi_{ab} \tag{13}$$

$$c_t = c_a + c_b \qquad \text{and} \qquad y = c_a/c_t$$

Analysis of the angular distribution of the intensity for low wavevector values and b = 0. In the small q limit, setting $P_i = 1 - q'^2R_{g,i}^2$ ($q'^2 = q^2/3$), equation (6) gives for $q'^2R_{g,i}^2 \ll 1$:

$$\frac{Kc_aM_a}{\Delta I(c, q \to 0)} = 1 + 2A_{2,a}M_ac_a + q'^2R_{g,a}^2 - \frac{4A_{2,ab}M_bc_ac_b(1 - q'^2R_{g,b}^2)}{1 + 2A_{2,b}M_bc_b(1 - q'^2R_{g,b}^2)} \tag{14}$$

Rearranging this equation slightly leads to:

$$\frac{Kc_aM_a}{\Delta I(c, q \to 0)} = A' + B'q'^2R_{g,a}^2 \tag{15}$$

with

$$A' = 1 + 2A_{2,a}M_ac_a - \frac{4A_{2,ab}^2M_aM_bc_ac_b}{1 + 2A_{2,b}M_bc_b} = \frac{Kc_aM_a}{\Delta I(c, q = 0)}$$

and

$$B' = 1 + \frac{4A_{2,ab}^2M_aM_bc_ac_b}{(1 + 2A_{2,b}M_bc_b)^2} \times \frac{R_{g,b}^2}{R_{g,a}^2}$$

Table 1 Molecular weight M_w, radius of gyration $R_{g,i}$, second virial coefficient $A_{2,i}$ and interaction parameter χ_i for the PS–PMMA mixtures

Polymer	M_w	Solvent	$R_{g,i}$ (Å)	$A_{2,i}$ ($\times 10^4$) (mol ml g^{-2})	χ_i
PS_1	135000	Benzene	136	5.6	0.442
PS_2	1.4×10^6	Toluene	660	2.8	0.465
		Benzene	660	3	0.469
$PMMA_1$	128000[a]	Dioxane	128	5.2	
		THF	115	4.9	0.439
		Ethyl acetate	107	2.8	
$PMMA_2$	1.3×10^6[a]	Dioxane	575	5.2	
		THF	540	2.0	0.475
		Ethyl acetate	470	1.2	
$PMMA_3$	3×10^6[a]	Dioxane	1000	1.9	
		THF	910	1.75	0.478
		Ethyl acetate	795	1.10	

[a]Average value in the three solvents

One can define an apparent radius of gyration as:

$$R^2_{g,app} = R^2_{g,a}B' = R^2_{g,a}\left[1 + \frac{4A^2_{2,ab}M_aM_bc_ac_b}{(1 + 2A_{2,b}M_bc_b)^2} \times \frac{R^2_{g,b}}{R^2_{g,a}}\right] \quad (16)$$

This apparent radius of gyration is determined from the slope of the variation of the quantity $Kc_aM_a/\Delta I(c, q)$ *versus* q'^2 in the small q range. It depends on the respective sizes of the two polymers; it is also strongly affected by the thermodynamic parameters $A_{2,b}$ and $A_{2,ab}$, as well as the concentrations of the polymers.

We can also define a radius of gyration of polymer A, $R_{g,a}(c)$, expressed by the more classic method, i.e. by normalizing relation (15) by the quantity $Kc_aM_a/\Delta I(c, q = 0)$, as follows:

$$\frac{Kc_aM_a}{\Delta I(c, q \to 0)} \times \frac{1}{A'} = 1 + \frac{B'}{A'}R^2_{g,a}q'^2$$

Thus $R_{g,a}(c)$ is given by the following relation:

$$R_{g,a}(c) = \frac{R_{g,a}}{Kc_aM_a/\Delta I(c, q = 0)} \times \left[1 + \frac{4A^2_{2,ab}M_aM_bc_ac_b}{(1 + 2A_{2,b}M_bc_b)^2} \times \frac{R^2_{g,b}}{R^2_{g,a}}\right]^{1/2} \quad (17)$$

This radius of gyration will be more affected by the thermodynamic properties, because the term for scattering at $q = 0$ appears in the expression.

EXPERIMENTAL

Samples. PS samples were prepared by anionic polymerization following the classical procedure used in the laboratory[11]. The polydispersity index M_w/M_n for these samples was in the range of 1.1–1.3.

The parameters such as molecular weight M_w, radius of gyration $R_{g,i}$ and second virial coefficient $A_{2,i}$, were determined by light scattering, and are reported in *Table 1* for PS–PMMA mixtures and in *Table 2* for PS–PVAc mixtures.

With PS, PMMA has been studied using four mixtures containing polymers with different molecular weights. The PMMA sample with a low molecular weight ($M_w = 128000$) was obtained by anionic polymerization ($M_w/M_n = 1.4$). The three other PMMA samples were fractions from a polymer obtained by radical polymerization ($M_w/M_n = \sim 1.4$–1.5).

Table 2 Molecular weight M_w, radius of gyration $R_{g,i}$, second virial coefficient $A_{2,i}$ and interaction parameter χ_i for the PS–PVAc mixtures

System	Polymer	M_w	$R_{g,i}$	$A_{2,i}$ ($\times 10^4$)	χ_i
S'_I	PS	130000	166	6.39	0.415
	PVAc	130000	218	5.71	0.442
S'_{II}	PS	245000	255	5.31	0.429
	PVAc	245000	334	4.88	0.444
S'_{III}	PS	396000	340	4.68	0.437
	PVAc	412000	456	5.84	0.443

The solvents used for the PS–PMMA mixtures were benzene and toluene, which are good solvents for both polymers. In these solvents the refractive index increment of PMMA is zero ($b = 0$). It is not possible to have direct access to the molecular characteristics of the PMMA samples by light scattering in these solvents because $b = 0$. Thus, the molecular parameters were determined in three other solvents, tetrahydrofuran (THF), ethyl acetate and dioxane, which give finite values of b. From these three solvents, we tried to select the one in which the thermodynamic properties of PMMA are as close as possible to those in benzene and toluene.

For this purpose the virial coefficient $A_{2,b}$, was measured by the osmotic pressure method on a PMMA sample with a $M_n = 180000$ and $M_w/M_n = 1.5$ in benzene. The value of $A_{2,b}$ obtained ($=4.4 \times 10^{-4}$) is then recalculated for our low molecular weight PMMA sample by considering the variation of A_2 with molecular weight[12] and the correction due to polydispersity[13]. The corrected value is close to that found by light scattering in THF. Therefore, we decided to consider the molecular characteristics of PMMA in THF (*Table 1*).

A commercial PVAc sample was treated in order to minimize the ramification degree by hydrolysis and reacetylization methods. The purified PVAc was fractionated to obtain samples with different molecular weights. Their characteristics are listed in *Table 2*.

Techniques. The experiments were carried out using a Fica 50 scattering apparatus with a vertically polarized incident beam. The scattering angles were varied from 30 to 150°. In order to explore a domain of $q^2R_g^2$ as large as possible, some of the measurements were performed at 365, 436 and 546 nm. The measurements at 365 nm allowed us to specify the behaviour of the scattered intensity at high $q^2R_g^2$.

The experiments were performed at room temperature at which the solvents are good for the polymers. The solutions were centrifuged at 25 000*g* for 2 h. The solvents were distilled twice.

RESULTS AND DISCUSSION

Thermodynamic properties: analysis of the scattered intensity at q = 0

Generally, in the semi-dilute regime and at the spinodal, the parameter determined experimentally is the quantity $A_{2,ab}$. The mutual interaction parameter χ_{ab} is then calculated by using equation (5), where the parameters χ_a and χ_b are assumed constant. In fact, some experiments realized by osmometry and light scattering on polymer–good solvent binary systems have shown that the parameter χ is practically constant. On the other hand, in dilute solutions and with the 'null average contrast' condition, the parameter χ_{ab} is directly obtained experimentally (cf. equations (12) and (13)).

PS–PMMA–benzene systems. The thermodynamic study was performed at a composition $y_a = 0.5$, where y_a is the ratio of the concentrations of component a and components a + b, for two systems:

S_I = PS (M_a = 135 000)–PMMA (M_b = 128 000) –benzene

S_{II} = PS ($M_a = 1.4 \times 10^6$)–PMMA ($M_b = 1.3 \times 10^6$) –benzene

These mixtures were studied over a wide range of concentrations (from dilute solution to onset of phase separation). *Figure 1* gives variations of $Kc_{PS}M_{PS}/\Delta I(c, q = 0)$ as a function of the PS concentration c_{PS}, and as a function of the total concentration c_t for S_{II}.

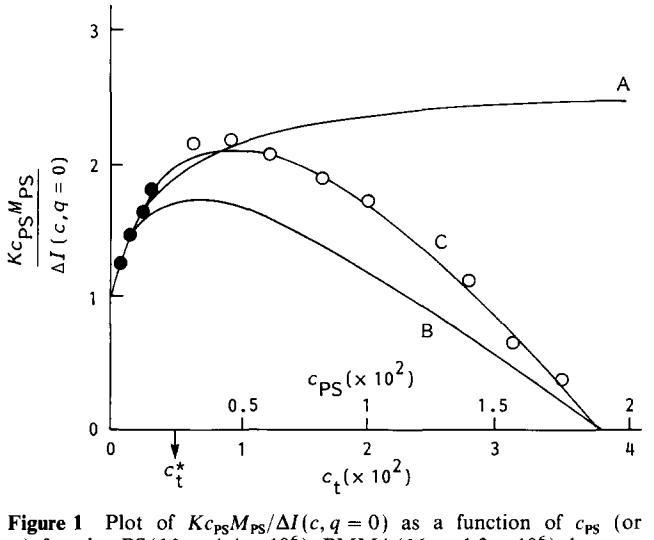

Figure 1 Plot of $Kc_{PS}M_{PS}/\Delta I(c, q = 0)$ as a function of c_{PS} (or c_t) for the PS($M_a = 1.4 \times 10^6$)–PMMA($M_b = 1.3 \times 10^6$)–benzene system. (●, ○) Experimental points (dilute solution and semi-dilute solution). (——) Calculated curves deduced from equation (6) with $A_{2,a} = 3 \times 10^{-4}$ and $A_{2,b} = 2 \times 10^{-4}$: (A) $A_{2,ab}^2 = A_{2,a}A_{2,b}$, ($\chi_{ab} = 0$); (B) $A_{2,ab} = 4.10 \times 10^{-4}$; (C) $A_{2,ab} = 1.43 \times 10^{-4} \times (c_t/c^*)^{0.38}$

(1) χ_{ab} *parameters values at the spinodal.* First, the χ_{ab} parameters have been calculated from the concentrations at the spinodal ($c_{PS} = 16.2 \times 10^{-2}$ g ml^{-1} for S_I and 3.82×10^{-2} g ml^{-1} for S_{II}), by considering equation (7) of the spinodal and equation (5) between the virial coefficients and the Flory interaction parameters (with $\varphi_S \neq 1$, $\varphi_S = 1 - \varphi_a - \varphi_b$, and χ_a and χ_b constant). We obtain $A_{2,ab} = 12.69 \times 10^{-4}$ for S_I and 4.1×10^{-4} for S_{II}, and thus the deduced values of the interaction parameters χ_{ab} are, respectively, 11.3×10^{-3} and 4.45×10^{-3}. We have compared the experimental variations of the ratio $Kc_{PS}M_{PS}/\Delta I(c, q = 0)$ with the calculated curve (equation (6)), taking the virial coefficients $A_{2,a}$, $A_{2,b}$ and $A_{2,ab}$ (value determined from the spinodal) as constant. This is shown in curve B in *Figure 1* for S_{II}. It appears that the calculated curve differs from the experimental data.

These two systems are less incompatible than the systems studied elsewhere, for example, PS–PDMS[5], PMMA–PDMS[7] or PS–polyisobutylene[4]. To estimate the degree of incompatibility of these various systems, one can compare the concentration at the spinodal c_{sp} of the symmetrical ($M_a = M_b$) mixtures with equivalent mass and for the same ratio of concentrations. This estimation is only a first approximation because c_{sp} depends on the mass of components, the ratio of concentration (or composition) and eventually the solvent. In fact, the real criterion is the prefactor of the scaling laws giving the variation of the χ_{ab} parameter or the critical concentration of demixing c_k with the molecular weight (c_k can be assimilated to c_{sp} for symmetrical systems[5]).

For both systems studied here, one could conceive a polymer concentration dependence of the terms $A_{2,ab}$ and χ_{ab} in semi-dilute solutions. Such observations have already been pointed out by Fukuda *et al.*[14] for the PS–PMMA–bromobenzene systems. They noticed that the parameter χ_{ab} was constant in dilute solution and increased with the polymer concentration beyond a concentration c^{**} higher than the overlap concentration c^* [$c^* = 3M/(4\pi R_g^3 N_a)$, $M = (M_a + M_b)/2$ and $R_g = (R_{g,a} + R_{g,b})/2$]. The concentration c^{**} can be defined as a 'cross-over' indicating a change of regime for χ_{ab}; χ_{ab} is constant for $c < c^{**}$ and increases with concentration if $c > c^{**}$.

(2) χ_{ab} *value in dilute solution.* The analysis of our experimental results does not allow the determination of the χ_{ab}^d parameter values in dilute solution with satisfactory precision because $\chi_{ab} \ll \chi_i$. This is shown in *Figure 1*, where curves A and B have been calculated with very different values (curve A, $\chi_{ab} = 0$ and curve B, $\chi_{ab} = 4.45 \times 10^{-3}$). At weak concentrations, these curves are practically identical.

The mixture PS–PMMA has been studied already in bromobenzene under the 'null average contrast' condition[14]. We have assumed that the benzene, toluene and bromobenzene are thermodynamically equivalent solvents for this mixture. This seems to be justified if one compares the values of the χ parameters given in *Table 1* (PS–toluene, PMMA–toluene) and in reference 14 (PS–bromobenzene).

One has, for example:

PS (M_w = 280 000)–bromobenzene $\chi = 0.455$

Table 3 Values of overlap concentration c^*, 'cross-over' concentration c^{**}, spinodal concentration c_t^{sp}, and the interaction parameter χ_{ab} and the second virial coefficient $A_{2,ab}$ in dilute solution and at the spinodal for PS–PMMA–benzene systems S_I and S_{II}

System	In dilute solution				At the spinodal		
	χ_{ab}^d ($\times 10^3$)	$A_{2,ab}^d$ ($\times 10^4$) (mol ml g^{-2})	c^* ($\times 10^2$) (g ml^{-1})	c^{**} ($\times 10^2$) (g ml^{-1})	c_t^{sp} ($\times 10^2$) (g ml^{-1})	χ_{ab}^{sp} ($\times 10^3$)	$A_{2,ab}^{sp}$ ($\times 10^4$) (mol ml g^{-2})
S_I $M_a = 135\,000$ $M_b = 128\,000$	4.84	5.46	2.46	5.7	16.2	11.3	12.69
S_{II} $M_a = 1.4 \times 10^6$ $M_b = 1.3 \times 10^6$	1.7	2.53	0.24	1.25	3.82	4.45	4.10

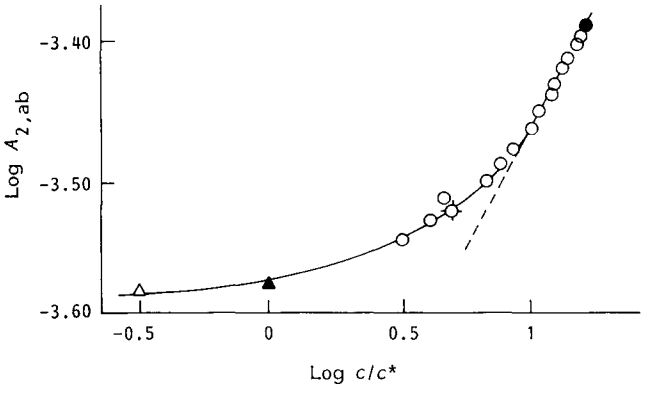

Figure 2 Variation of $A_{2,ab}$ *versus* c/c^* for the system PS(1.4×10^6)–PMMA(1.3×10^6)–benzene: (△) dilute solution; (▲) at c^*; (-◇-) at c^{**}; (●) at the spinodal

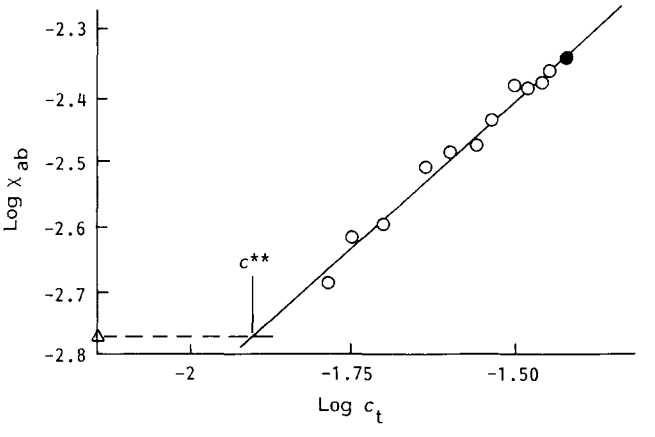

Figure 3 Variation of χ_{ab} as a function of c_t for the system PS(1.4×10^6)–PMMA(1.3×10^6)–benzene: (△) dilute solution; (●) at the spinodal

PS ($M_w = 135\,000$)–toluene $\chi = 0.442$

PMMA ($M_w = 210\,000$)–bromobenzene $\chi = 0.454$

PMMA ($M_w = 180\,000$)–toluene $\chi = 0.441$

(The value for the PMMA–toluene systems is obtained by osmometry.)

Under these conditions, χ_{ab} can be determined from the scaling law which relates it to the molecular weight[15] in dilute solution as follows:

$$\Delta A_{2,ab} = \frac{\tilde{v}^2}{2V_S}\chi_{ab} = 4.15 \times 10^{-3} M_w^{-0.45} \qquad (18)$$

with $$\Delta A_{2,ab} = A_{2,ab} - \frac{A_{2,a} + A_{2,b}}{2}$$

and $$\tilde{v} = \frac{\tilde{v}_a + \tilde{v}_b}{2} \qquad (19)$$

The parameters χ_{ab}^d and $A_{2,ab}^d$ determined in this way are given in *Table 3*.

(3) χ_{ab} *dependence on polymer concentration in semi-dilute solution.* At concentrations beyond the overlap concentration c^*, and from experimental data of the $KM_{PS}c_{PS}/\Delta I(c, q = 0)$ ratio as a function of the concentration, we have calculated the $A_{2,ab}(c)$ generalized parameters using the following relation:

$$A_{2,ab}^2(c) = \left(1 + 2A_{2,a}M_a c_a - \frac{KM_a c_a}{\Delta I(c, q = 0)}\right) \times \left(\frac{1 + 2A_{2,b}M_b c_b}{M_a M_b c_t^2}\right) \qquad (20)$$

with $c_a = c_b = c_t/2$.

The $A_{2,i}$ and $A_{2,ab}$ parameters are considered as varying with concentration ($\varphi_a \neq 1$), while the χ_a and χ_b parameters are constant in equation (5).

The $A_{2,ab}$ values are plotted as a function of the c/c^* ratio for the system S_{II}, in a double logarithmic representation, in *Figure 2*. One can see that for concentrations higher than c^*, $A_{2,ab}(c)$ increases strongly with a linear variation and obeys the empirical relation:

$$A_{2,ab}(c) = 1.434 \times 10^{-4}(c/c^*)^{0.38} \qquad (21)$$

We likewise obtain a linear increase in χ_{ab} with concentration, which gives the value for χ_{ab}^d in dilute solution at a concentration $c^{**} = 1.25 \times 10^{-2}$ g ml^{-1} as indicated in *Figure 3* ($= 5.2c^*$).

A similar analysis for the system S_I, which has a lower molecular weight, leads to:

$$A_{2,ab}(c) = 4.61 \times 10^{-4}(c/c^*)^{0.53} \qquad (22)$$

where

$$c^{**} = 5.7 \times 10^{-2} \text{ g ml}^{-1} \quad \text{and} \quad c^{**} = 2.3c^*.$$

For PS–PMMA–bromobenzene, Fukuda *et al.*[14] observed the change in the behaviour of χ_{ab} at $c^{**} = 3.3c^*$, and for molecular weights from 245 000 to 2.3×10^6, in contrast to our results. In fact, it is important to remember that for our systems the value of χ_{ab}^d in dilute solution was not directly accessible. Its estimation in bromobenzene could lead to uncertainty in the determination of c^{**}.

PS–PVAc–styrene systems. For these systems, the experiments were performed in the 'null average contrast' condition.

Three systems with different molecular weight were studied:

S'_I = PS (M_a = 120 000)–PVAc (M_b = 120 000)–styrene

S'_{II} = PS (M_a = 240 000)–PVAc (M_b = 240 000)–styrene

S'_{III} = PS (M_a = 396 000)–PVAc (M_b = 412 000)–styrene

The 'null average contrast' is verified for a weight composition approximately equal to 0.5 at $q = 0$. The variation of the quantity $c_t/\Delta I(c, q = 0)$ as a function of the total concentration c_t for S'_{II} is shown in *Figure 4* (curve A). Two different domains exist: one domain in dilute solution for which $c_t/\Delta I(c, q = 0)$ varies linearly with c_t with a small slope; and one domain beyond a concentration c^{**} in which this ratio decreases rapidly and tends to zero at the spinodal concentration.

(1) χ^d_{ab} *in dilute solution and* χ_{ab} *at the spinodal.* The experimental conditions being those of the 'null average contrast' condition, meant that the χ^d_{ab} values could easily be calculated with a good precision from the slope of the straight line of $Kc_t/\Delta I(c, q = 0)$ as a function of c_t, at concentrations lower than c^{**} (equations (12) and (13)). The χ^d_{ab} parameters for the three mixtures are listed in *Table 4*, as well as the corresponding second virial coefficients $A^d_{2,ab}$. As has been shown in reference 15, these parameters depend on molecular weight in dilute solution. $A_{2,ab}$ and χ_{ab} determined at the spinodal using equation (7) are three times higher than in dilute solution (*Table 4*).

(2) χ_{ab} *dependence on concentration in semi-dilute solution.* In semi-dilute solution, the variations of $A_{2,ab}$ and of χ_{ab} *versus* c_t have been determined in a similar way as the analysis of the PS–PMMA mixtures, i.e. using the experimental curve which gives the variations of the ratio $K'c_t/\Delta I(c, q = 0)$ as a function of c_t. From a theoretical point of view, this variation can be expressed using the general equation (1), by:

$$\frac{K'c_t}{\Delta I(c, q = 0)} = \frac{1 + 2A_{2,a}M_a y c_t + 2A_{2,b}M_b(1 - y)c_t + \alpha c_t^2}{a^2 M_a y + b^2 M_b(1 - y) + \beta c_t} \quad (23)$$

with

$$\alpha = 4(A_{2,a}A_{2,b} - A^2_{2,ab})M_a M_b y(1 - y)$$

$$\beta = 2(a^2 A_{2,b} + b^2 A_{2,a} - 2abA_{2,ab})M_a M_b y(1 - y)$$

Figure 5 shows the variation of $A_{2,ab}$ and *Figure 6* that of χ_{ab} as a function of c_t at concentrations higher than the overlap concentration c^*. These curves are relative to the system S'_{II}. The two other systems present the same behaviour except that the 'cross-over' concentration c^{**} changes. The empirical expressions for $A_{2,ab}$ derived therefrom are:

$$S'_I: A_{2,ab}(c) = 2.44 \times 10^{-3} c_t^{0.32}$$

$$S'_{II}: A_{2,ab}(c) = 2.22 \times 10^{-3} c_t^{0.33} \quad (24)$$

$$S'_{III}: A_{2,ab}(c) = 2.15 \times 10^{-3} c_t^{0.33}$$

The c^{**} concentrations extrapolated from *Figure 6* and

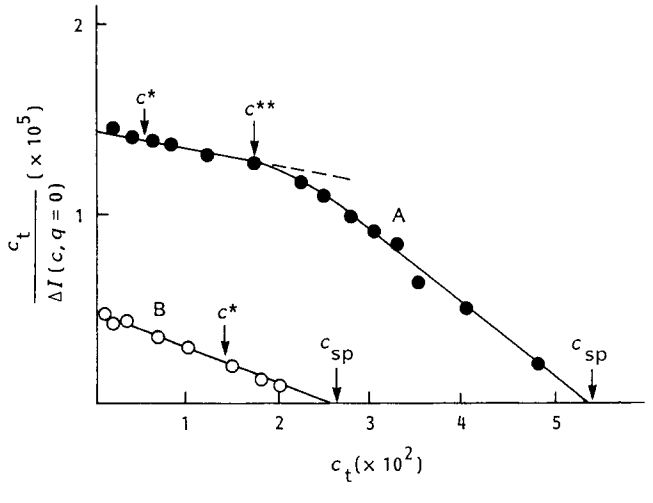

Figure 4 Plot of $c_t/\Delta I(c, q = 0)$ as a function of c_t under the 'null average contrast' condition for two systems: (A) PS(240 000)–PVAc-(240 000)–styrene; (B) PS(230 000)–PDMS(240 000)–toluene[5]

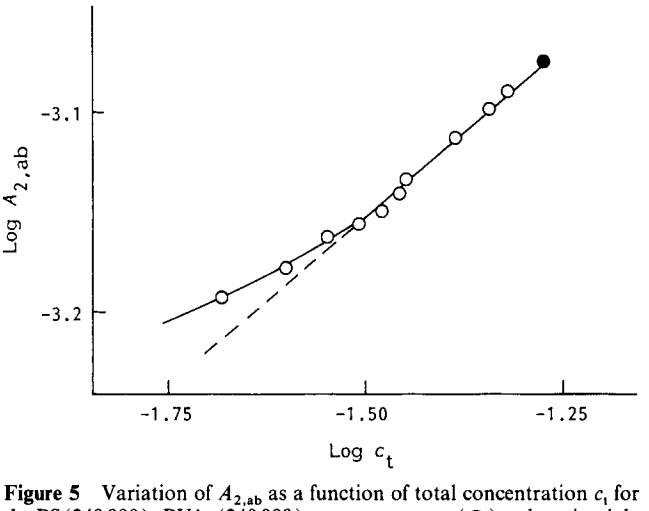

Figure 5 Variation of $A_{2,ab}$ as a function of total concentration c_t for the PS(240 000)–PVAc(240 000)–styrene system: (●) at the spinodal

Table 4 Values of overlap concentration c^*, 'cross-over' concentration c^{**}, spinodal concentration c_t^{sp}, and the interaction parameters χ_{ab} and the second virial coefficient $A_{2,ab}$ in dilute solution and at the spinodal for PS–PVAc–styrene systems S'_I, S'_{II} and S'_{III}

System	In dilute solution				At the spinodal		
	χ^d_{ab} ($\times 10^3$)	$A^d_{2,ab}$ ($\times 10^4$) (mol ml g^{-2})	c^* ($\times 10^3$) (g ml^{-1})	c^{**} ($\times 10^3$) (g ml^{-1})	c_t^{sp} ($\times 10^2$) (g ml^{-1})	χ^{sp}_{ab} ($\times 10^3$)	$A^{sp}_{2,ab}$ ($\times 10^4$) (mol ml g^{-2})
S'_I M_a = 130 000 M_b = 128 000	5.7	6.4	6.4	19.05	6.8	19.14	10.29
S'_{II} M_a = 245 000 M_b = 245 000	4.3	5.66	3.7	15.49	5.3	16.86	8.44
S'_{III} M_a = 396 000 M_b = 412 000	3.4	5.27	2.4	7.08	3.4	11.02	7.06

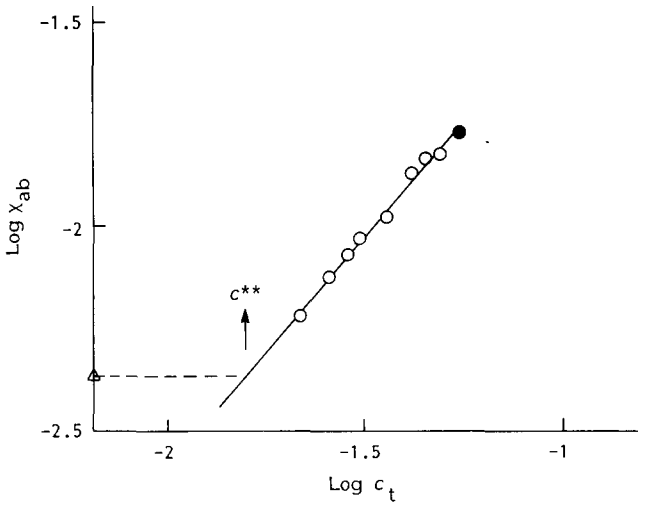

Figure 6 Variation of χ_{ab} as a function of total concentration c_t for the PS(240 000)–PVAc(240 000)–styrene system: (△) dilute solution; (●) at the spinodal

listed in *Table 4* lead to the following relation for all systems:

$$c^{**} \simeq 3.5(\pm 0.5)c^{*} \qquad (25)$$

Discussion of the two systems. For both systems presented here, the χ_{ab} parameter is constant in dilute solution and, may be, at the beginning of the semi-dilute regime (this depends on the definition of c^*) and has a concentration dependence when the concentration is higher than c^{**} ($c^{**} = 3$–$4c^*$). Note that the PS–PDMS–toluene system[5] does not show this 'cross-over' behaviour concerning χ_{ab}. This is shown in *Figure 4* (curve B), where we have plotted the quantity $KM_ac_a/\Delta I(c, q = 0)$ *versus* c_t. Here χ_{ab} is constant from dilute solution up to the onset of phase separation. This is explained if we suppose that c^{**} is equal to $3c^*$ or $4c^*$ for all systems, while the critical concentration c_k is higher than c^{**} for the PS–PMMA and PS–PVAc systems ($c_k \sim 8$–$10c^*$), and less than c^{**} for the PS–PDMS system ($c_k \sim 2c^*$)[15]. In other words, for the PS–PDMS–solvent system which is more incompatible, phase separation is reached before c^{**}.

The curves shown in *Figure 3* for the PS–PMMA–toluene system and in *Figure 6* for the PS–PVAc–styrene system indicate a linear variation of χ_{ab} with concentration (for $c > c^{**}$) in a log–log representation. If we consider the data of the various systems, we obtain:

$$\chi_{ab} \sim \varphi^{0.6\pm 0.05} \qquad \text{(PS–PMMA–toluene)}$$

$$\chi_{ab} \sim \varphi^{0.7\pm 0.1} \qquad \text{(PS–PVAc–styrene)}$$

where φ is the total volume fraction of polymer.

For the PS–PMMA mixture in bromobenzene studied elsewhere[14], it has been reported that the slope of the curve log χ_{ab} *versus* log φ is not constant, but varies with φ, the values of the slope being always higher than 0.5.

It should be noted that the experimental value of the exponent is higher than the theoretical value predicted by De Gennes[16] (0.25). This discrepancy has already been discussed in reference 14.

Apparent dimensions: the angular distribution of scattered light

The analysis concerning the PS–PMMA–toluene systems is performed under two experimental conditions: constant composition by weight ($y = c_a/c_a + c_b = 0.5$, i.e. for $c_a/c_b = 1$); and constant concentration c_b of PMMA such that the quantity $2A_{2,b}M_bc_b = 1$.

The Zimm plots are very similar to those obtained for the PS–PDMS system[5]. At constant composition the variation of $Kc_aM_a/\Delta I$ as a function of q^2 is linear with a slope increasing with concentration. At constant concentration c_b, one observes a distortion in the diagram characterized by a curvature in the small q range.

Analysis at the small q limit. (1) *Constant composition.* The two mixtures studied in this case are:

S_I = PS ($M_a = 135\,000$)–PMMA ($M_b = 128\,000$) –benzene

S_{II} = PS ($M_a = 1.4 \times 10^6$)–PMMA ($M_b = 1.3 \times 10^6$) –benzene

Figures 7 and *8* show the evolution of the $R_{g,app}/R_{g,a}(0)$ ratio (curve A), and that of the $R_{g,a}(c)/R_{g,a}(0)$ ratio (curve B) as a function of c_{PS}, respectively, for S_I and S_{II}. The points represent the experimental results, and the solid lines the theoretical curves which are deduced from the relations:

$$\frac{R_{g,app}}{R_{g,a}(0)} = \left[1 + \frac{4A_{2,ab}^2M_aM_by(1-y)c_t^2}{[1 + 2A_{2,b}M_b(1-y)c_t]^2} \times \frac{R_{g,b}^2}{R_{g,a}^2}\right]^{1/2} \qquad (26)$$

and

$$\frac{R_{g,a}(c)}{R_{g,a}(0)} = \frac{1}{\left[\dfrac{Kc_aM_a}{\Delta I(c, q=0)}\right]} \times \left[1 + \frac{4A_{2,ab}^2M_aM_bc_ac_b}{(1 + 2A_{2,b}M_bc_b)^2} \times \frac{R_{g,b}^2}{R_{g,a}^2}\right]^{1/2} \qquad (27)$$

The term $A_{2,ab}$ used for the calculations are those determined from the analysis of the intensity at $q = 0$,

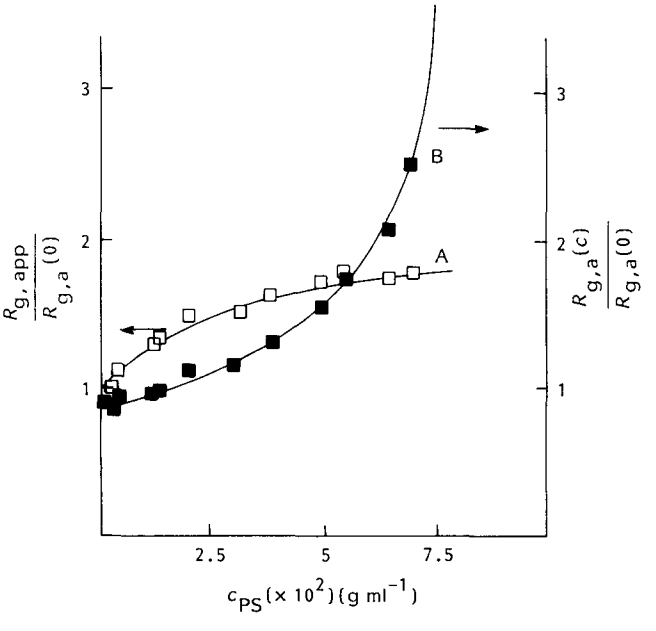

Figure 7 Variation of $R_{g,app}/R_{g,a}(0)$ (curve A), and $R_{g,a}(c)/R_{g,a}(0)$ (curve B) *versus* c_{PS} for the PS(135 000)–PMMA(128 000)–toluene system at $y = 0.5$. (——) Calculated curves with $A_{2,ab} = 4.61 \times 10^{-4}(c/c^*)^{0.53}$

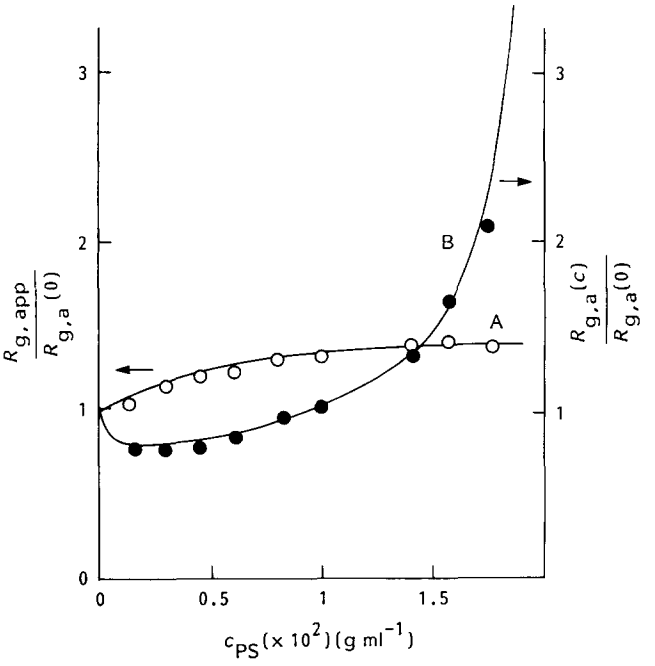

Figure 8 Variation of $R_{g,app}/R_{g,a}(0)$ (curve A), and $R_{g,a}(c)/R_{g,a}(0)$ (curve B) *versus* c_{PS} for the PS(1.4×10^6)–PMMA(1.3×10^6)–benzene system at constant composition $y = 0.5$. (——) Calculated curves with $A_{2,ab} = 1.434 \times 10^{-4}(c/c^*)^{0.38}$

and are given as a function of the concentration of the polymer by equations (21) and (22). The $A_{2,b}$ term is given by equation (5), where the volume fraction φ_S is different from unity ($\varphi_S = 1 - \varphi_a - \varphi_b$, where $\varphi_a = c_a\tilde{v}_a$ and $\varphi_b = c_b\tilde{v}_b$) and Flory's parameter χ_b is considered to be constant. The $R_{g,a}$ and $R_{g,b}$ values are those obtained in binary dilute solutions (*Table 1*). Under these conditions, the agreement between theory and experiment is good.

Like the PS–PDMS–THF[5] systems, the interpretation of the angular distribution of the scattered intensity seems to be well explained by the theory elaborated by Benoit and Benmouna[9], when the polymer composition is constant.

(2) *Constant and low concentration in PMMA* ($2A_{2,b}M_bc_b = 1$). The results are from two PS–PMMA–toluene mixtures:

S_{II} = PS ($M_a = 1.4 \times 10^6$)–PMMA ($M_b = 1.3 \times 10^6$) –toluene

S_{III} = PS ($M_a = 1.4 \times 10^6$)–PMMA ($M_b = 3 \times 10^6$) –toluene

The main molecular characteristics are given in *Table 1*. The PMMA concentration is such that $A_{2,b}M_bc_b = 1$, and c_{PS} varies from 0.54×10^{-3} to 8.19×10^{-3} g ml^{-1}.

The experimental results for S_{III} are given by the points in *Figure 9*, i.e. by plotting the ratio $Kc_{PS}M_{PS}/\Delta I(c,q)$ *versus* q^2 for different concentrations. Distortions appear in this plot becoming more pronounced as c_{PS} increases.

The analysis in the low qR_g range allows us to evaluate the apparent radius of gyration $R_{g,app}$ as a function of c_{PS}. These radii increase strongly with concentration, as shown in *Table 5*. This increase is explained qualitatively by the theoretical equation (16). For a more quantitative interpretation, the $A_{2,ab}$ term has first to be determined from the experimental results at $q = 0$: $A_{2,ab} = 2.48 \times 10^{-4}$ for S_{II} and $A_{2,ab} = 2.32 \times 10^{-4}$ for S_{III}. Furthermore, it is necessary to introduce in equation (16) the extrapolated value of $R_{g,PS}$ in ternary and infinitely dilute system, and to take into account a decrease of $R_{g,PMMA}$ for the sample of high molecular weight. These values are:

$S_{II} = R_{g,PS} = 620$ Å and $R_{g,PMMA} = 540$ Å

$S_{III} = R_{g,PS} = 580$ Å and $R_{g,PMMA} = 760$ Å

The calculated values of $R_{g,app}$ are practically the same as the experimental values (*Table 5*). Therefore, in the case where the PMMA concentration is constant, it is necessary to take account of the generalized form factors depending on the polymer concentration. It also means that the PS molecules introduced in a matrix containing molecules of toluene and PMMA contract, i.e. $R_{g,PS}$ extrapolated at $c_{PS} \to 0$ is lower than that determined for binary systems. This result has already been described in detail by Kuhn and Cantow[17] and also confirms the calculations of renormalization by Nose[18].

Intermediate q *range* ($qR_g > 1$ *and* $2A_{2,b}M_bc_b = 1$). (1) *Evolution of* ΔI^{-1} *as a function of* q^2. The distortions in *Figure 9* are the result of a different behaviour in $\Delta I^{-1}(c,q)$ with the wavevector range considered.

For the low q range, the experimental variations of ΔI^{-1} *versus* $\sin^2\theta/2$ or q^2 are represented by straight lines with slopes increasing with c_{PS}. On the other hand, in the high q range, these variations tend to have an asymptotic behaviour. The quantitative analysis can be performed using equation (6) giving the quantity $KM_{PS}c_{PS}/\Delta I(c,q)$ as a function of q^2. The form factors can be expressed by the Debye equation[19]:

$$P_i = \frac{2}{u^2}[\exp(-u) + u - 1] \qquad (28)$$

where $u = q^2R_{g,i}^2$ with $R_{g,i}$ determined at low wavevectors in the ternary systems. The calculated curves are

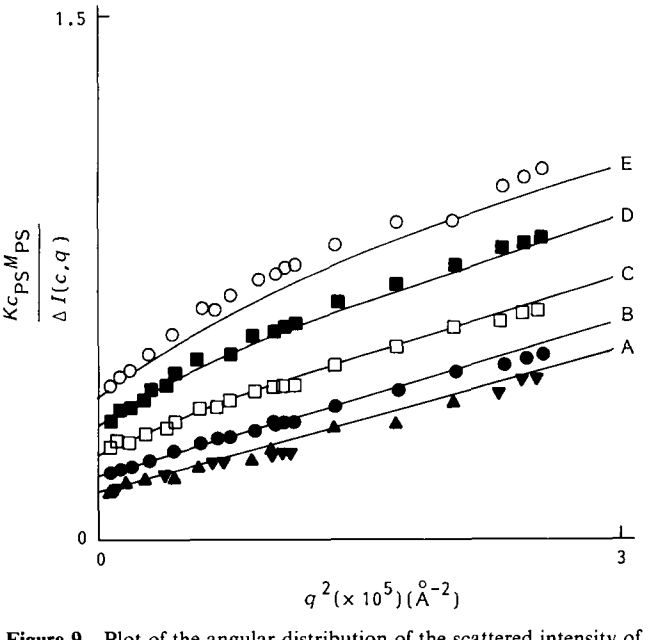

Figure 9 Plot of the angular distribution of the scattered intensity of the PS(1.4×10^6)–PMMA(3×10^6)–toluene system for different concentrations of PS ($2A_{2,b}M_bc_b = 1$; $\lambda = 546$ and 365 nm). Points represent the experimental data and the solid lines the calculated curves: c_{PS} = (A) 0.54×10^{-3}; (B) 1.94×10^{-3}; (C) 3.74×10^{-3}; (D) 6.09×10^{-3}; (E) 8.19×10^{-3} g ml^{-1}

Table 5 Apparent radii of gyration *versus* PS concentration for PS–PMMA–toluene systems S_{II} and S_{III} with $2A_{2,ab}M_bc_b = 1$

S_{II} ($M_{PS} = 1.4 \times 10^6$, $M_{PMMA} = 1.3 \times 10^6$)				S_{III} ($M_{PS} = 1.4 \times 10^6$, $M_{PMMA} = 3 \times 10^6$)				
c_{PS} ($\times 10^3$) (g ml^{-1})	$y = \frac{c_{PS}}{c_{PS} + c_{PMMA}}$	$R_{g,app}$[a] (Å)	$R_{g,app}$[b] (Å)	c_{PS} ($\times 10^3$) (g ml^{-1})	$y = \frac{c_{PS}}{c_{PS} + c_{PMMA}}$	$R_{g,app}$[a] (Å)	$R_{g,app}$[c] (Å)	$R_{g,app}$[d] (Å)
0	–	620	–	0	–	580	–	–
2.2	0.59	740	736	0.54	0.26	624	654	632
4.13	0.73	805	811	0.85	0.36	651	693	660
6.03	0.79	905	879	1.24	0.45	680	735	694
8.12	0.84	990	948	1.66	0.52	695	786	728
				1.94	0.56	747	815	750
				3.74	0.71	890	985	880
				6.09	0.80	1067	1170	1025
				8.19	0.84	1137	1313	1138

[a]Experimental values
[b]Calculated values with $R_{g,PS} = 620$ Å and $R_{g,PMMA} = 540$ Å
[c]Calculated values with $R_{g,PMMA} = 910$ Å
[d]Calculated values with $R_{g,PMMA} = 760$ Å

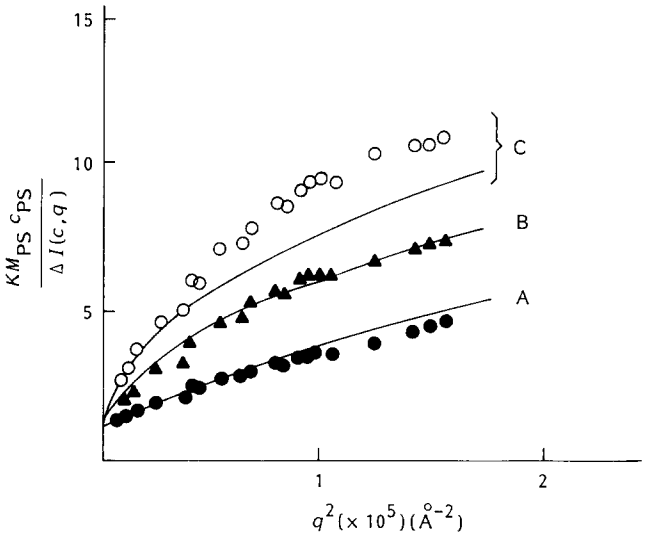

Figure 10 Plot of the angular distribution of the scattered intensity of the PS(1.4 × 10^6)–PDMS(4.2 × 10^6)–THF system for different concentrations of PS ($2A_{2,b}M_bc_b = 1$; $\lambda = 546$ and 436 nm). Points represent the experimental data and the solid lines the calculated curves: c_{PS} = (A) 1.58 × 10^{-3}; (B) 5.02 × 10^{-3}; (C) 7.535 × 10^{-3} g ml^{-1}

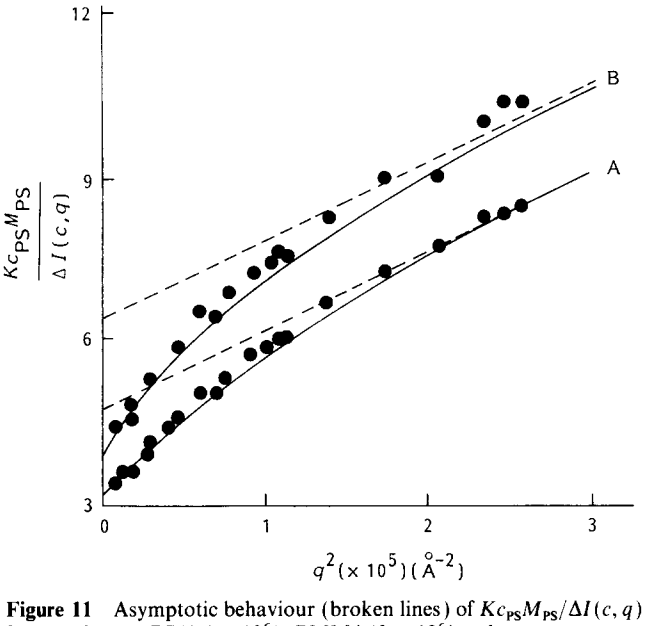

Figure 11 Asymptotic behaviour (broken lines) of $Kc_{PS}M_{PS}/\Delta I(c,q)$ for the PS(1.4 × 10^6)–PMMA(3 × 10^6)–toluene system ($2A_{2,b}M_b \sim 1$): c_{PS} = (A) 6.09 × 10^{-3}; (B) 8.019 × 10^{-3} g ml^{-1}

represented by the solid lines in *Figure 9*. A good agreement is obtained between the theoretical curves and the experimental points at low concentrations; a divergence exists when c_{PS} is high (8.19 × 10^{-2} g ml^{-1}).

We have reproduced in *Figure 10* the PS–PDMS–THF results reported in reference 5 and made under similar conditions

$$(M_{PS} = 1.4 \times 10^6, M_{PDMS} = 4.2 \times 10^6, 2A_{2,ab}M_bc_b = 1).$$

One observes the same features as above with more pronounced divergence at higher c_{PS}. At present, we do not have a satisfactory explanation for this divergence; some complementary experiments are required.

(2) *Asymptotic behaviour of* $\Delta I^{-1}(q)$. In *Figures 9* and *10*, ΔI^{-1} tends to an asymptotic limit in the intermediate q range. In the q range where $qR_{g,i} \gg 1$, the form factors $P_i(q)$ tend to an asymptotic limit proportional to $1/q^2R_{g,i}^2$. By substitution of this limit in equation (1), one can see that the scattered intensity is simply the superposition of the intensities corresponding to constituents A and B. In the case where one polymer has a vanishing refractive index increment, this limit corresponds to the scattered intensity by the 'visible' polymer only.

Therefore, in the high q range, the scattered intensity is not affected by the interaction properties of the polymers.

We now consider the expression $P_i(q)$ (equation (28)). For high qR_g values[20]:

$$P_i(q) = \frac{2}{u_i}\left(1 - \frac{1}{u_i}\right) \tag{29}$$

so that

$$P_i^{-1}(q) = \frac{u_i}{2}\left(1 + \frac{1}{u_i}\right) \tag{30}$$

In our case, when $dn/dc_b = 0$, the asymptotic behaviour

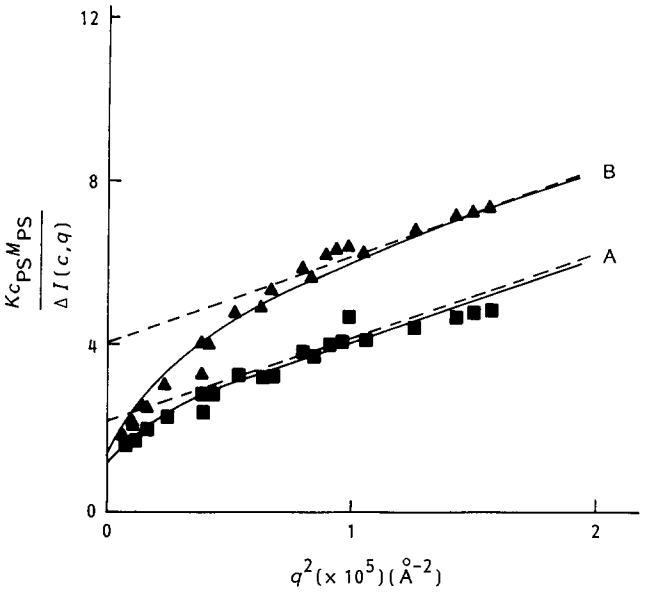

Figure 12 Asymptotic behaviour (broken lines) of $Kc_{PS}M_{PS}/\Delta I(c, q)$ for the PS(1.4×10^6)–PDMS(4.2×10^6)–THF system[5] ($2A_{2,b}M_b c_b \sim 1$): c_{PS} = (A) 1.58×10^{-3}; (B) 5.02×10^{-3} gml^{-1}

will depend only on the parameters related to PS. Then the relation is:

$$\frac{KM_{PS}c_{PS}}{\Delta I(qR_g \gg 1)} = P_{PS}^{-1} + 2A_{2,PS}M_{PS}c_{PS} \qquad (31)$$

Introducing in this relation P_{PS}^{-1} from equation (30), we have plotted in *Figures 11* and *12* the asymptotic limits (broken lines) for the PS–PMMA and PS–PDMS[5] systems. We note that the asymptotic behaviour is effectively reached at $q^2R_g^2 \gg 1$ for low c_{PS} values.

CONCLUSIONS

We have presented light scattering investigations of two systems (PS–PMMA–benzene or toluene and PS–PVAc–styrene) from dilute solutions up to the onset of phase separation. The thermodynamic study has shown similarities in incompatibility between the unlike polymers for both systems; they are less incompatible than other systems such as PS–PDMS–good solvent. For the systems studied here, χ_{ab} is constant in dilute solution and increases with polymer concentration above a cross-over concentration which seems three or four times higher than the overlap concentration.

A study of the angular distribution of the scattered intensity in the case of two PS–PMMA–toluene mixtures has allowed us to deduce that the apparent dimensions are very sensitive to the properties of the two polymers, and an asymptotic behaviour is reached at high $q^2R_g^2$.

ACKNOWLEDGEMENTS

The authors are very grateful to Professor H. Benoit for fruitful discussions and to Mrs M. Mottin for her technical assistance.

REFERENCES

1 Stockmayer, W. H. *J. Chem. Phys.* 1950, **18**, 58
2 Stockmayer, W. H. and Stanley, H. E. *J. Chem. Phys.* 1950, **18**, 153
3 Kratochvil, P., Vorliecek, J., Strakova, D. and Tuzar, Z. *J. Polym. Sci., Polym. Phys. Edn.* 1975, **13**, 2321
4 Van den Esker, M. W. J. and Vrij, A. *J. Polym. Sci., Polym. Phys. Edn.* 1976, **14**, 1943
5 Ould-Kaddour, L. and Strazielle, C. *Polymer* 1987, **28**, 459
6 Ould-Kaddour, L. and Strazielle, C. *Eur. Polym. J.* 1988, **24**, 117
7 Anasagasti, M. S., Katime, I. and Strazielle, C. *Makromol. Chem.* 1987, **188**, 201
8 Benoit, H. and Benmouna, M. *Polymer* 1984, **25**, 1059
9 Benoit, H. and Benmouna, M. *Macromolecules* 1984, **17**, 535
10 Fukuda, T., Nagata, M. and Inagaki, H. *Macromolecules* 1984, **17**, 548
11 Lapp, A., Beinert, G. and Picot, C. *Makromol. Chem.* 1984, **185**, 453
12 Cotton, J. P. *J. Phys. Lett.* 1980, **41**, 231
13 Yamakawa, H. 'Modern Theory of Polymer Solutions', Harper and Row, New York, 1971, Ch. 7
14 Fukuda, T., Nagata, M. and Inagaki, H. *Macromolecules* 1986, **19**, 1411
15 Ould-Kaddour, L., Anasagasti, M. S. and Strazielle, C. *Makromol. Chem.* 1987, **188**, 2223; Ould-Kaddour, L. and Strazielle, C. *Polym. Prepr.* 1988, **29**, 387
16 De Gennes, P. G. 'Scaling Concepts in Polymer Physics', Cornell University Press, Ithaca, Ch. 1
17 Kuhn, R. and Cantow, H. J. *Makromol. Chem.* 1969, **122**, 65
18 Nose, T. *J. Phys.* 1986, **45**, 517
19 Debye, P. *J. Appl. Phys.* 1947, **18**, 51
20 Des Cloiseaux, J. and Jannink, G. 'Les Polymères en Solution', Editions de Physique, 1987, Ch. XII